Korean J. Chem. Eng., 32(6), 1164-1169 (2015)
DOI: 10.1007/s11814-014-0305-y

pISSN: 0256-1115
eISSN: 1975-7220

Kinetics of thermal decomposition of ε-hexanitrohexaazaisowurtzitane by TG-DSC-MS-FTIR

Yan-Li Zhu†, Ming-Xin Shan, Zhi-Xia Xiao, Jing-Si Wang, and Qing-Jie Jiao

State Key Laboratory of Explosive Science and Technology, Beijing Institute of Technology, South Street No. 5, Zhongguancun, Haidian District, Beijing 100081, China
(*Received 6 May 2014 • accepted 8 October 2014*)

Abstract−Thermal decomposition of ε-hexanitrohexaazaisowurtzitane (HNIW) was studied by thermogravimetry-differential scanning calorimetry-mass spectrometry-Fourier transform infrared spectroscopy (TG-DSC-MS-FTIR) simultaneous analysis. It has been shown that there is a crystal transition point for ε-HNIW, and only a single decomposition process has been observed for HNIW. The kinetic parameters of thermal decomposition of HNIW were obtained by Kissinger and Flynn-Wall-Ozawa methods, indicating that HNIW has the higher reactivity compared to the other nitramines. The HNIW decomposition mechanism demonstrated by the non-isothermal kinetics conformed to Avrami-Erofeev equation with the factor of nucleus growth of n=1/3 and the conversion degree of α from 0.1 to 0.7. The MS and FTIR analyses indicated that the thermal decomposition of HNIW favors N-N bond cleavage over C-N bond cleavage as the rate determining step.

Keywords: Thermal Decomposition, Hexanitrohexaazaisowurtzitane, Explosive, Chemical Kinetics

INTRODUCTION

Thermal analysis is a useful technique for the characterization of energetic material [1,2]. The knowledge of the complex physicochemical processes involved in the thermal decomposition of explosives is essential from the practical point of view since it relates to the stability of these materials and may also be involved in the combustion and explosion processes [3]. The chemical decomposition mechanism, kinetic parameters and thermodynamic properties are the key factors in understanding the thermal decomposition of explosives [2]. The thermal analysis techniques have the advantage that a small amount of sample is required to yield sufficient information for the accurate determination of kinetic parameters for the thermal reaction quickly [4].

A relatively new energetic material, 2,4,6,8,10,12-hexanitro-2,4,6,8,10,12-hexaaza-tetracyclo-[5.5.0.0^{5,9}.0^{3,11}]-dodecane (HNIW), also known as CL-20, a multi-nitramine caged compound, has high energetic density, good chemical stability and better performance than cyclotetramethylenetetranitramine (HMX), which has been widely applied in various composite explosives and propellants [5]. HNIW is considered as the most powerful elementary explosive. It is predicted that HNIW would be a substitute for HMX, and equipped in various weapons very soon [6]. The thermal decomposition of HNIW has been investigated using molecular dynamics simulations [7-9] and different analytical instruments including thermogravimetry (TG), dynamic vacuum stability test (DVST), differential scanning calorimetry (DSC), mass spectrometry (MS), Fourier transform infrared spectroscopy (FTIR) and accelerating rate calorimetry (ARC) [3,5,10-13]. Although so much research has been carried out on thermal decomposition of HNIW mentioned above, studies based on TG-DSC coupled with MS-FTIR have not been reported. In addition, the originality of HNIW is revealed in the existence of different polymorphs [14], and ε-HNIW is considered the best crystal form with a better performance and lower sensitivity [15]. In the present study, a set of specific experimental devices of TG-DSC-MS-FTIR simultaneous system was used to study the thermal decomposition of ε-HNIW. The kinetic parameters were computed using two equations of Kissinger and Ozawa, based on variable heating rate. The purpose of this study is to gain insight into the detailed decomposition kinetic process of ε-HNIW.

EXPERIMENTAL

1. Materials and Characterization

Raw HNIW was brought from Qingyang chemical industry corporation, Liaoning Province. The HNIW sample, used here, was obtained by the recrystallization of raw HNIW, using ethyl acetate as solvent and petroleum ether as anti-solvent. The details about the preparation procedures can be found elsewhere [16,17]. The average size of the recrystallized product was 80 μm (Fig. 1). The polymorph of product was confirmed to be ε-HNIW by field emission scanning electron microscope (FE-SEM, Hitachi S-4800, Japan) and X-ray diffraction (XRD, Bruker D4, Cu Kα).

2. Thermal Analysis

A TG-DSC-MS-FTIR coupling system composed of a Netzsch STA449C (Selb, Germany), Netzsch-QMS403C (Selb, Germany) and Nicolet 6700 FTIR (Madison, WI) was used for thermal analysis. The ionizing electron energy of Netzsch-QMS403C is 70 eV. The pressure injection of the quartz capillary gas connector is 1 bar and the capillary temperature is 200 °C. The resolution of Nico-

†To whom correspondence should be addressed.
E-mail: zhuyanli1999@bit.edu.cn

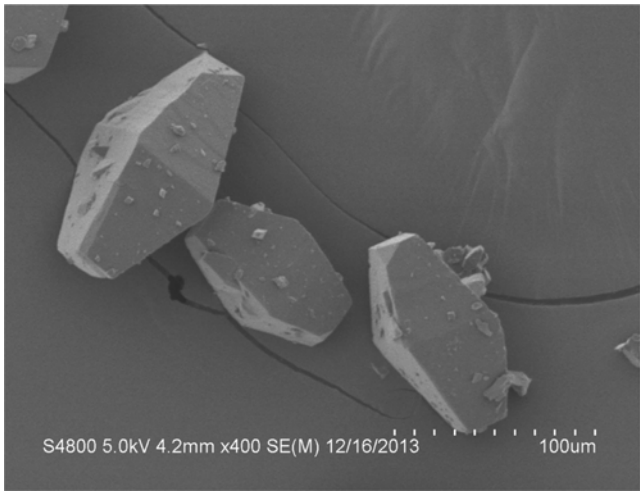

Fig. 1. SEM image of ε-HNIW.

let 6700 FTIR is 4 cm^{-1}. The quartz capillary gas connector is used. The gas cell and gas tube between TG-DSC and FTIR stay at 200 °C.

About 1 mg of a sample was placed in an alumina crucible with a pinhole on the lid and heated from 30 to 500 °C. α-Al_2O_3 was used as the reference sample. High-purity argon was used with a gas flow rate of 20 mL min^{-1}.

Non-isothermal thermal decomposition of ε-HNIW was performed at the rates of 5, 10, 15 and 20 °C min^{-1}. The non-isothermal data can be used to obtain some kinetic parameters [18], and they were processed by Kissinger and Flynn-Wall-Ozawa methods. The thermal decomposition process of ε-HNIW was monitored by MS and FTIR on-line with the heating rate of 10 °C min^{-1}. The MS and FTIR results can provide some information about the produced gases and chemical reactions occurring during thermal decomposition.

RESULTS AND DISCUSSION

1. TG-DSC Analysis

The TG curves of ε-HNIW at the heating rates of 5, 10, 15 and 20 °C min^{-1} shown in Fig. 2 indicate that there is only one mass loss step for thermal decomposition of HNIW regardless of the heating rate. This is not consistent with Turcotte and his co-workers' results, which were that the observed behavior of the mass loss curves confirmed a two-step decomposition for ε-HNIW [13]. This discrepancy may be due to the particle size of the sample [14,19]. The crystal size and the size distribution both influence the thermolysis of HNIW. Fig. 2 shows that the onset and end temperatures were increased with increasing the heating rate. An average mass loss of about 81% was recorded after the experiments and small amounts of black residue were produced. This residue may contain C=O, C=N, and NH groups [12].

Fig. 3 shows that the onset of exothermic decomposition in DSC curve at 10 °C min^{-1} occurred at the same temperature as the onset of mass loss in the TG curve. The DSC curve shows a thermogram for ε-HNIW has a broad endothermic peak of about 172 °C, which is ascribed to the phase transition from $\varepsilon \rightarrow \gamma$ polymorphs since there was no change in the mass of ε-HNIW [20]. One exotherm with peak maximum temperature of about 249 °C, which occurred at the same temperature as the peak of mass loss in the derivative thermogravimetry (DTG) curve (not shown here), is assignable to thermal decomposition of γ-HNIW or the mixture of ε-HNIW and γ-HNIW, corresponding to the mass loss step in the TG curve. The endothermic peak changed little with increasing the heating rate, while the exothermic peak shifted to the high temperature side and the exothermic enthalpy became larger, indicating the rate of the thermal decomposition of HNIW is increased at larger heating rate. The characteristic temperatures of thermal decomposition process of HNIW at various heating rates are summarized in Table 1.

Kissinger and Flynn-Wall-Ozawa methods, described in the fol-

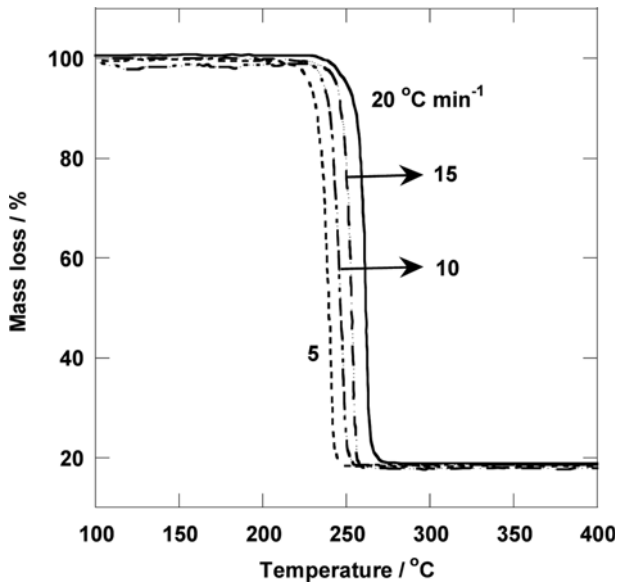

Fig. 2. TG curves of thermal decomposition of ε-HNIW at heating rates of 5, 10, 15 and 20 °C min^{-1}.

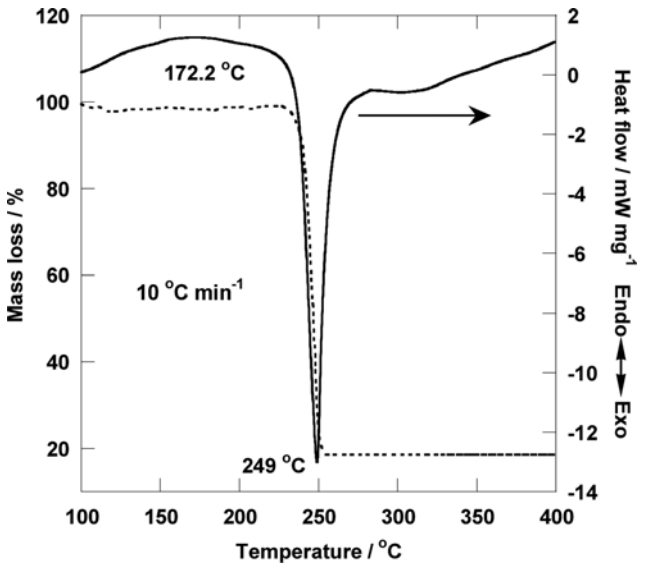

Fig. 3. TG-DSC curves of thermal decomposition of ε-HNIW at 10 °C min^{-1}.

Table 1. Temperatures and kinetic parameters of thermal decomposition of HNIW at different heating rates

Heating rate [°C min^{-1}]	T_o [°C]	T_e [°C]	T_p [°C]	E_K [KJ mol^{-1}]	lg (A_K/s^{-1})	r_K	E_O [KJ mol^{-1}]	r_O
5	219.3	245.9	241.2	174.6	17.19	0.997	172.8	0.998
10	225.1	253.1	249.0					
15	231.5	257.4	254.8					
20	240.4	262.6	258.3					

T_o-Onset temperature of thermal decomposition of HNIW, T_e-End temperature of thermal decomposition of HNIW, T_p-Peak temperature of thermal decomposition of HNIW, r-linear correlation coefficient

lowing Eqs. (1) and (2), respectively, were used to gain the first insight into the decomposition process of ε-HNIW. The non-isothermal TG-DTG data at 5, 10, 15, and 20 °C min^{-1} were used to calculate the apparent activation energy E and pre-exponential factor A.

Kissinger method (differential method) [1]:

$$\ln\left[\frac{\beta}{T_p^2}\right]=\ln\frac{A_K R}{E_K}-\frac{E_K}{R}\frac{1}{T_p} \quad (1)$$

Flynn-Wall-Ozawa method (integral method) [21]:

$$\lg\beta=\lg\left(\frac{AE_O}{RG(\alpha)}\right)-2.315-0.4567\frac{E_O}{RT} \quad (2)$$

where β is the heating rate, T_p is the peak temperature of DTG curve, A_K and A are the pre-exponential factor, E_K and E_O are the apparent activation energy determined by Kissinger and Ozawa methods, respectively; R is the gas constant, T is the absolute temperature and the temperature of DTG curve, α is the conversion degree, which is the mass ratio of the reacted substance to the raw, and $G(\alpha)$ is the integral mechanism function.

The DTG peak temperatures of ε-HNIW at the various heating rates are summarized in Table 1. The values of E_K, A_K, E_O and r (the relating linear correlation coefficient) obtained by Kissinger's and Ozawa's methods are also given in Table 1. The values of $E_{\alpha,i}$ at various conversion degree α_i calculated by Ozawa method is given in Fig. 4. It shows that the value of E, which is about 170 kJ mol^{-1}, has changed little with $0.1<\alpha<0.7$. Therefore, it is reasonable to investigate the decomposition mechanism in this range.

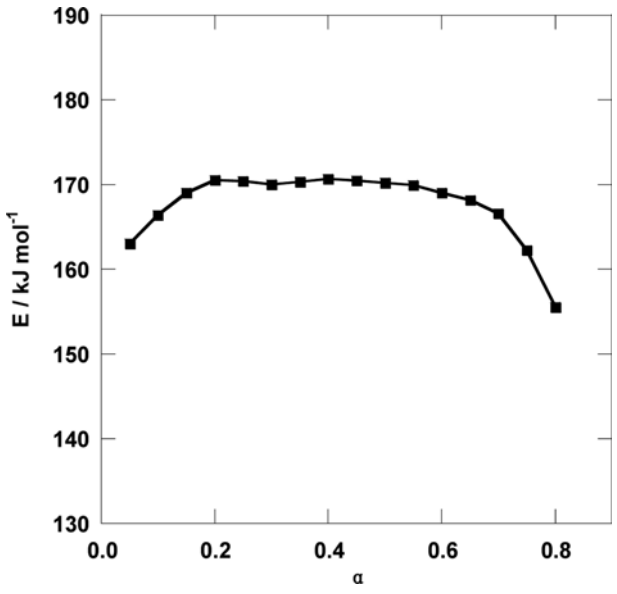

Fig. 4. Dependence of $E_{\alpha,i}$ on α_i curve for HNIW.

Four kinds of integration method (Ordinary integral [22], Mac-Callum-Tanner [23], Coats-Redfern [24] and Šatava-Sesták [25]) and one differential method [26] were introduced to determine the most probable kinetic model function, $G(\alpha)$, which was selected from 41 types of kinetic model functions in Hu et al [22]. Each kinetic model function and the original TG-DTG data at various heating rates in Table 1 were put into the above five equations to calculate the values of E, A, r and Q (standard mean square deviation). Some statistical criteria, like r and Q, were applied to decide the most probable mechanism function, $G(\alpha)$. The values of A and E obtained by Eqs. (1) and (2) were also applied to evaluate the validity of $G(\alpha)$.

The results indicated that the thermal decomposition process of ε-HNIW can be described as Avrami-Erofeev equation: $G(\alpha)=[-\ln(1-\alpha)]^{1/3}$ or $f(\alpha)=3(1-\alpha)[-\ln(1-\alpha)]^{2/3}$. It is suggested that this process is controlled by the nucleation and subsequent growth. This is consistent with the results reported by Kim and his coworkers [27]. The kinetic equation is $d\alpha/dt=3*10^{17.2}(1-\alpha)[-\ln(1-\alpha)]^{2/3}e^{-2.1*10^4/T}$ (where t is the time.) with the factor of nucleus growth n=1/3. The activation energies of the thermal decomposition of ε-HNIW are close to those of the other nitramines, whereas the pre-exponential in the case of ε-HNIW is higher, which determines the higher reactivity of this substance, indicating the substantial role of the entropy contribution to the kinetics of this reaction [10].

2. MS-FTIR Analysis

The non-isothermal thermal decomposition process of HNIW was monitored by MS and FTIR on-line with the heating rate of 10 °C min^{-1}. Fig. 5 represents the mass spectra of the gaseous products from HNIW decomposition, which shows the m/z 14, 16, 17, 18, 26, 27, 28, 29, 30, 32, 43, 44, 45, 46 and 52 were detected. The onset, peak and end temperatures for the main ion numbers and the possible assignments are summarized in Table 2.

The FTIR of the gaseous products of HNIW decomposition is presented in Fig. 6 at the time when the intensity of FTIR series is the maximum. The temperature is about 244 °C. Compared with the MS results in Fig. 5, it is certain that there are N_2O (1,274 cm^{-1}), NO_2 (1,644 cm^{-1} and 1,525 cm^{-1}), HCN (737 cm^{-1}), NO (1,916 cm^{-1}), CH_2O (1,734 cm^{-1}), HNCO (2,265 cm^{-1}) and the wavenumbers for H_2O and CO_2 [28]. FTIR spectra show that the main gaseous products for thermal decomposition of HNIW are N_2O, NO_2, HCN and CH_2O. The ion current intensity of m/z 46 (NO_2) shown in Fig. 5 is not strong, probably due to the bombardment of ion source

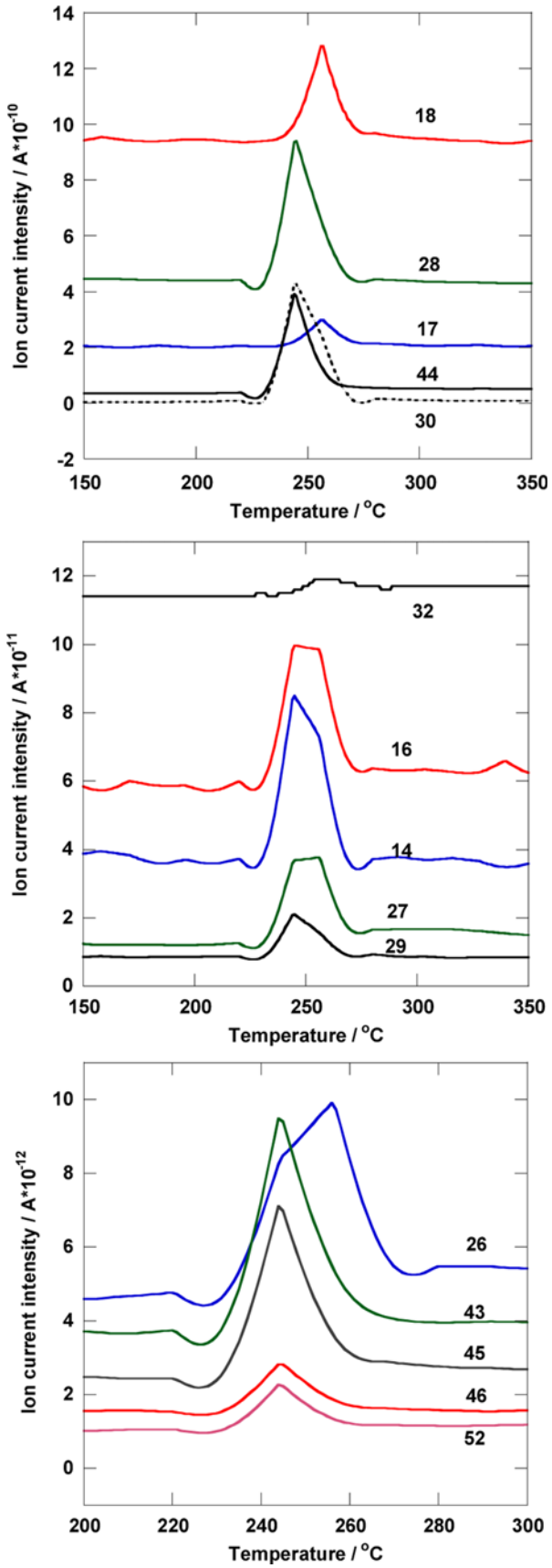

Fig. 5. MS of gaseous products of HNIW at heating rate of 10 °C min^{-1}.

Table 2. m/z Ratio and the corresponding temperatures (T_o-T_p-T_e)

m/z	Possible assignment	T_o-T_e [°C]	T_p [°C]
14	CH_2^+, N^+	226.9-272.7	244.2, 256.1
16	O^+, CH_4^+, NH_2^+	226.9-275.9	244.3, 256.1
17	NH_3, OH^+	234.0-272.0	256.3
18	H_2O, NH_4^+	238.0-276.0	256.3
26	CN^+	226.9-275.0	244.3, 256.3
27	HCN, $C_2H_3^+$	226.9-273.7	244.1, 256.1
28	CO^+, N_2^+, CH_2N^+	227.0-275.0	244.3
29	CHO^+	226.9-274.7	244.2
30	NO, CH_2O, C_2H_6, N_2H_2	229.0-274.0	244.2
32	O_2, H_2NO, N_2H_4	240.0-283.0	256.2
43	HNCO, N_2CH_3	226.9-273.7	244.3
44	CO_2, N_2O, C_2H_4O	226.9-268.9	243.9
45	HCO_2, HN_2O, NH_2CHO	226.9-265.0	244.2
46	NO_2, C_2H_6O, HCOOH	226.9-264.9	243.9
52	C_2N_2	226.9-265.0	243.9

by MS and changing NO_2^+ into NO^+ and O^+.

Two types of reaction pathways are suggested for the initial thermal decomposition of cyclic nitramines: (i) ring-opening reactions accompanied by a concerted C-N bond ring fission, (ii) homolytic cleavage of a N-N bond accompanied by the elimination of the -NO_2 group [3]. Brill and his co-workers [29] believed that there is a competition between these two pathways for thermal decomposition of cyclic nitramines. In the case of RDX, the first detected primary products are CH_2O and N_2O if the initial reaction pathway is a concerted C-N bond ring fission, and HCN and HONO for the N-N bond cleavage [30]. It is proposed that similar types of decomposition steps for HNIW, since it belongs to the same class of cyclic nitramine compounds. Fig. 5 and Table 2 show that the m/z number of 27 for ε-HNIW is detected at about 226.9 °C, while m/z 30 is at 229.0 °C. Since m/z 27 and m/z 30 may be assigned to HCN and CH_2O, respectively, it is speculated that the decomposition of the cage appeared to commence with the loss of nitro groups via cleavage of N-N bond, followed by breaking of C-N and C-C bonds [12]. This is supported by the activation energy of about 170 kJ mol^{-1}, calculated by Kissinger method and described above, which virtually coincides with the E_a values for other reactions involving the cleavage of N-NO_2 [10]. The homolysis of N-N bond weakens the C-N bond and makes it to be oxidized to C=O or carbonyl-containing compound, while nitro may be reduced to N_2O [12]. Therefore, it is inferred that N_2O and NO_2 are produced simultaneously. This is confirmed by the MS results, as shown in Table 2. C-N bond breaking led to the formation of substituted pyrazine derivatives, which further decomposed to lower molecular mass fragment such as H_2O, CO, NO, NH_3 and HNCO [3].

CONCLUSIONS

The kinetics of thermal decomposition of ε-HNIW was analyzed by TG-DSC-MS-FTIR. The thermal decomposition of ε-HNIW should be considered as the decomposition of γ-HNIW or the mixture of ε-HNIW and γ-HNIW since ε-HNIW can convert to γ-HNIW

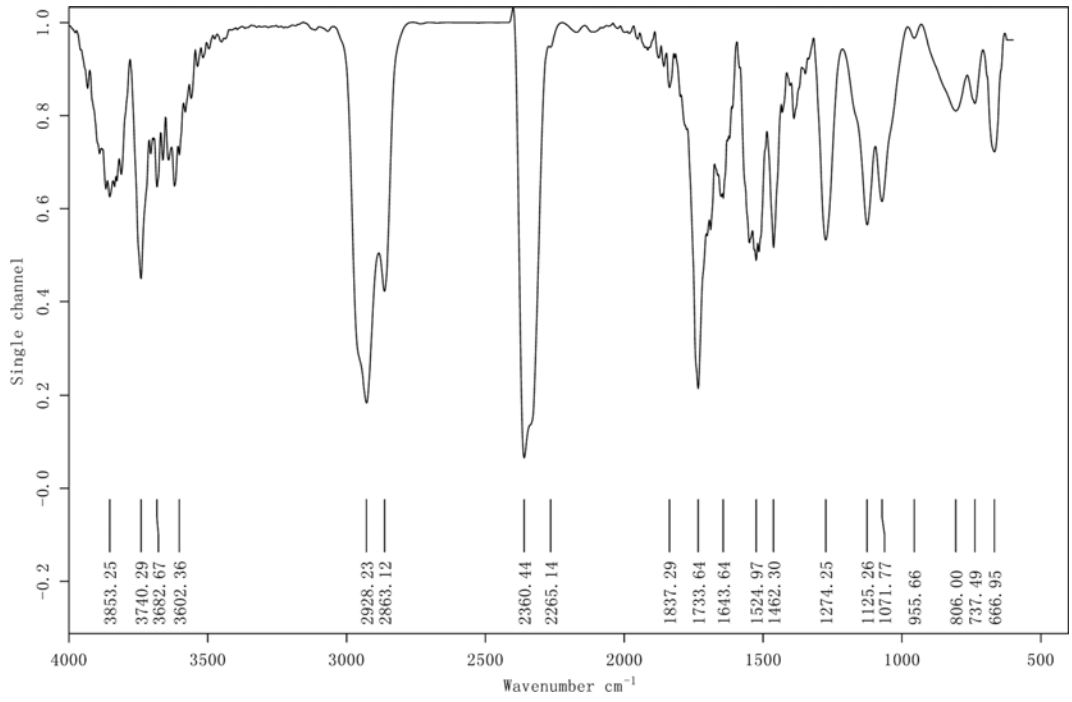

Fig. 6. FTIR plots of gas products of HNIW at 244 °C.

when heated to about 172 °C. The activation energy of thermal decomposition of ε-HNIW, calculated by Kissinger and Ozawa methods was about 170 kJ mol^{-1}, which corresponds to the dissociation energy of N-N bond. The non-isothermal kinetics results showed that the thermal decomposition reaction mechanism function for ε-HNIW conformed to Avrami-Erofeev equation with the factor of nucleus growth n=1/3. Based on the published data and the present study, it is assumed that the homolytic cleavage of the $N\text{-}NO_2$ bond is the primary act of ε-HNIW decomposition.

ACKNOWLEDGEMENTS

The authors would like to appreciate the financial support from National Natural Science Foundation of China (Grant No. 51304024 and No. 11172042).

REFERENCES

1. H. E. Kissinger, *Anal. Chem.*, **29**, 1702 (1957).
2. J.-S. Lee and K.-S. Jaw, *J. Therm. Anal. Calorim.*, **85**(2), 463 (2006).
3. N. H. Naika, G. M. Gorea, B. R. Gandheb and A. K. Sikder, *J. Hazard. Mater.*, **159**, 630 (2008).
4. G. Liptay, J. Nagy, A. Borbély-Kuszmann and J. Ch. Weil, *J. Therm. Anal. Cal.*, **32**, 1683 (1987).
5. R. Liu, Z. Zhou, Y. Yin, L. Yang and T. Zhang, *Thermochim. Acta*, **537**, 13 (2012).
6. X.-L. Xing, F.-Q. Zhao, S.-N. Ma, S.-Y. Xu, L.-B. Xiao, H.-X. Gao and R.-Z. Hu, *J. Therm. Anal. Calorim.*, **110**, 1451 (2012).
7. S. Okovytyy, Y. Kholod, M. Qasim, H. Fredrickson and J. Leszczynski, *J. Phys. Chem. A.*, **109**(12), 12964 (2005).
8. X . Xu, H. Xiao, J. Xiao, W. Zhu, H. Huang and J. Li, *J. Phys. Chem. B.*, **110**, 7203 (2006).
9. D. C. Sorescu and B. M. Rice, *J. Phys. Chem. B.*, **102**(6), 948 (1998).
10. B. L. korsounskii, V. V. Nedelko, N. V. Chukanov, T. S. Larikova and F. Volk, *Russ. Chem. Bull.*, **49**(5), 812 (2000).
11. R. Yang, H. An and H. Tan, *Combust. Flame*, **135**, 463 (2003).
12. D. G. Patil and T. B. Brill, *Combust. Flame*, **87**, 145 (1991).
13. R. Turcotte, M. Vachon, Q. S. M. Kwok, R. Wang and D. E. G. Jones, *Thermochim. Acta*, **433**, 105 (2005).
14. V. V. Nedelko, N. V. Chukanov, A. V. Raevskii, B. L. Korsounskii, T. S. Larikova and O. I. Kolesova, *Propellants, Explosives, Pyrotechnics*, **25**, 255 (2000).
15. Q.-L. Yan, S. Zeman, A. Elbeih and Z.-W. Song, *J. Therm. Anal. Calorim.*, **112**, 823 (2013).
16. X. Jiang, X. Guo, H. Ren , Y. Zhu and Q. Jiao, *J. Chem. Eng. Jpn.*, **45**(6), 380 (2012).
17. X. Jiang, X. Guo, H. Ren and Q. Jiao, *Central European Journal of Energetic Materials*, **9**(3), 139 (2012).
18. Y. L. Ren, B. W. Cheng, J. S. Zhang, A. B. Jiang and W. L. Fu, *Chem. Res. Chinese Universities*, **24**(5), 628 (2008).
19. Ch. An, X. Geng and J. Wang, *Sci. Tech. Energetic Materials*, **73**(5-6), 175 (2012).
20. S. Löbbecke, M. A. Bohn, A. Pfeil and H. Krause, 29th International Annual Conference of ICT, 145, Karlsruhe, Germany (1998).
21. T. Ozawa, *J. Therm. Anal.*, **2**, 301 (1970).
22. R. Z. Hu, S. L. Gao, F. Q. Zhao, Q. Z. Shi, T. L. Zhang and J. J. Zhang, *Thermal analysis kinetics*, Second Ed., Beijing, Science Press (2008) (In Chinese).
23. J. R. MacCallum and J. Tanner, *Eur. Polym. J.*, **6**, 907 (1970).
24. A. W. Coats and J. P. Redfern, *Nature*, **201**, 68 (1964).
25. V. Šatava and J. J. Šesták, *J. Therm. Anal.*, **8**, 477 (1975).
26. Z. Q. Yang, R. Z. Hu, Y. J. Liang and X. D. Li, *Acta Phys. Chim. Sinica*,

2(1), 13 (1986).
27. J. H. Kim and Y. J. Yim, *J. Chem. Eng. Jpn.*, **32**(2), 237 (1999).
28. P. J. Brush, *Temperature Jump/Fourier transform Infrared Spectroscopy: A Noval Method for Investigation the Chemistry of a Burning Surface*, University of Delaware (1993).
29. S. T. Thynell, P. E. Gongwer and T. B. Brill, *J. Propul. Power*, **12**(5), 933 (1996).
30. Y.-L. Zhu, H. Huang, H. Ren and Q.-J. Jiao, *J. Energy Mater.*, **31**, 178 (2013).